





## 25 Abstract

26 Mollusks record valuable information in their hard parts that reflect ambient environmental  
27 conditions. For this reason, shells can serve as excellent archives to reconstruct past climate and  
28 environmental variability. However, animal physiology and biomineralization, which are often  
29 poorly understood, can make the decoding of environmental signals a challenging task. Many of  
30 the routinely used shell-based proxies are sensitive to multiple different environmental and  
31 physiological variables. Therefore, the identification and interpretation of individual environmental  
32 signals (e.g. water temperature) often is particularly difficult. Additional proxies not influenced by  
33 multiple environmental variables or animal physiology would be a great asset in the field of  
34 paleoclimatology. The aim of this study is to investigate the potential use of structural properties  
35 of *Arctica islandica* shells as an environmental proxy. A total of eleven specimens were analyzed  
36 to study if changes of the microstructural organization of this marine bivalve are related to  
37 environmental conditions. In order to limit the interference of multiple parameters, the samples  
38 were cultured under controlled conditions. Three shells presented here were grown at two different  
39 water temperatures (10 °C and 15 °C) for multiple weeks and exposed only to ambient food  
40 conditions. An additional eight specimens were reared under three different dietary regimes. Shell  
41 material was analyzed with two techniques: (1) Confocal Raman microscopy (CRM) was used to  
42 quantify changes of the orientation of microstructural units and pigment distribution and (2)  
43 Scanning electron microscopy (SEM) was used to detect changes in microstructural organization.  
44 Our results indicate that *A. islandica* microstructure is not sensitive to changes in the food source,  
45 and likely, shell pigment are not altered by diet. However, seawater temperature had a statistically  
46 significant effect on the orientation of the biomineral. Although additional work is required, the



47 results presented here suggest that the crystallographic orientation of biomineral units of *A.*  
48 *islandica* may serve as an alternative and independent proxy for seawater temperature.

49

50

## 51 1. Introduction

52 Biomineralization is a process through which living organisms produce a protective, mineralized  
53 hard tissue. The considerable diversity of biomineralizing species contributes to high variability in  
54 terms of shape, organization and mineralogy of the structures produced (Lowenstam and Weiner,  
55 1989; Carter et al., 2012). Different architectures at the micrometer and nanometer scale and  
56 different biochemical compositions determine material properties that serve specific functions  
57 (Weiner and Addadi, 1997; Currey, 1999; Merkel et al., 2007). Besides these differences, all  
58 mineralized tissues are hybrid materials consisting in hierarchical arrangements of biomineral units  
59 surrounded by organic matrix, also known as “microstructures” (Bøggild, 1930; Carter and Clark,  
60 1985; Rodriguez-Navarro et al., 2006) or “ultrastructures” (Blackwell et al., 1977; Olson et al.,  
61 2012) or overall “fabrics” (Schöne, 2013; Schöne et al., 2013). The carbonate and organic phases  
62 represent the fundamental level of the organization of biomaterials (Aizenberg et al., 2005; Meyers  
63 et al., 2006). The mechanisms of microstructure formation and shaping, especially in mollusks, has  
64 attracted increasing attention during recent decades. At present, it is commonly accepted that the  
65 organic compounds play an important role in the formation of the inorganic phases of biominerals  
66 (Weiner and Addadi, 1991; Berman et al., 1993; Dauphin et al., 2003; Nudelman et al., 2006).  
67 However, the identification of the exact mechanisms driving biomineralization is still an open  
68 research question. Previous studies conducted on mollusks show that environmental parameters



69 can influence microstructure formation (Lutz, 1984; Tan Tiu and Prezant, 1987; Tan Tiu, 1988;  
70 Nishida et al., 2012). These results set the stage for a research interest toward the use of shell  
71 microstructures as proxies for reconstructing environmental conditions (Tan Tiu, 1988; Tan Tiu  
72 and Prezant, 1989; Olson et al., 2012; Milano et al., 2015).

73 Mollusks are routinely used as climate and environmental proxy archives because they can  
74 record a large amount of environmental information in their shells (Richardson, 2001; Wanamaker  
75 et al., 2011a; Schöne and Gillikin, 2013). Whereas structures at nanometric level are still  
76 underexplored as potential environmental recorders, shell patterns at lower magnification, such as  
77 individual growth increments, are commonly used for this purpose (Jones, 1983; Schöne et al.,  
78 2005; Marali and Schöne, 2015; Mette et al., 2016). Mollusks deposit skeletal material on a  
79 periodic basis and at different rates (Thompson et al., 1980; Deith, 1985). During periods of fast  
80 growth, growth increments are formed whereas during periods of slower growth, growth lines are  
81 formed (Schöne, 2008; Schöne and Gillikin, 2013). The periodicity of such structures ranges from  
82 tidal to annual (Gordon and Carriker, 1978; Schöne and Surge, 2012). By crossdating time-series  
83 with similar growth patterns it is possible to construct century and millennia-long master  
84 chronologies (Marchitto et al., 2000; Black et al. 2008; Black et al., 2016; Butler et al., 2013). This  
85 basic approach, in combination with geochemical methods, has great potential in reconstructing  
86 past climatic conditions (Wanamaker et al., 2011b). At present, the most frequently used and well-  
87 accepted geochemical proxy is oxygen isotopic composition of shell material ( $\delta^{18}\text{O}_{\text{shell}}$ ) (Epstein,  
88 1953; Grossman and Ku, 1986; Schöne et al., 2004; Wanamaker et al., 2007) which may serve as  
89 a paleothermometer and/or paleosalinometer (Mook, 1971; Andrus, 2011); however, the  $\delta^{18}\text{O}_{\text{shell}}$   
90 is influenced by both seawater temperature and the isotopic composition of seawater ( $\delta^{18}\text{O}_{\text{water}}$ ;  
91 related to salinity). Thus,  $\delta^{18}\text{O}_{\text{shell}}$ -based temperature reconstructions are particularly challenging  
92 in habitats with fluctuating  $\delta^{18}\text{O}_{\text{water}}$  conditions such as estuaries or restricted basins (Gillikin et al.,



93 2005). Because of the multiple impacts on  $\delta^{18}\text{O}_{\text{shell}}$  values, there have been substantial efforts  
94 (including elemental ratios; cite Schone et al 2010 papers here) to develop alternative techniques  
95 to reconstruct environmental variables from mollusk shells.

96 This study investigates the possibility using shell microstructure properties to serve as a new  
97 environmental proxy. For this purpose, the effects of seawater temperature (grown at 10 °C and 15  
98 °C) and dietary regime on the microstructural units of *Arctica islandica* cultured under controlled  
99 conditions were analyzed and quantified. *A. islandica* was chosen as model species because of its  
100 great potential in paleoclimatology and paleoceanography (see Schöne, 2013; Wanamaker et al.,  
101 2016). Its extreme longevity of up to more than 500 years makes this species a highly suitable  
102 archive for long-term paleoclimate and environmental reconstructions (Schöne et al., 2005;  
103 Wanamaker et al., 2008; Wanamaker et al., 2012; Butler et al., 2013).

104

105

106

## 107 2. Materials and Methods

108 The analyses were conducted on eleven *A. islandica* shells. Three juvenile *A. islandica* shells,  
109 sampled for the seawater temperature experiment, were collected alive on November 21, 2009  
110 aboard the *F.V. Three of a Kind* off Jonesport, Maine USA (44° 26' 9.829"N, 67° 26' 18.045"W)  
111 in 82 m water depth. From 2009 to 2011, all animals were kept in a flowing seawater laboratory at  
112 the Darling Marine Center, Walpole, Maine, USA (see Beirne et al., 2012 for additional details).  
113 In 2011, clams were grown at two different temperature regimes for 16 weeks (Table 1). At the  
114 completion of the experiment, shells were estimated to be between 4 to 5 years old. Eight one-year



115 old juveniles were collected in July 2014 from Kiel Bay, Baltic Sea (54° 32' N, 10° 42' E; Fig. 1)  
116 and kept alive in tanks at 7 °C for six months at the Alfred Wegener Institute for Polar and Marine  
117 Research (AWI), Bremerhaven, Germany. During this time interval, the animals were fed with an  
118 algal mix of *Nannochloropsis* sp., *Isochrysis galbana* and *Pavlova lutheri*. Then, they were  
119 transferred to the Royal Netherlands Institute for Sea Research (NIOZ), Texel, The Netherlands,  
120 and cultured in tanks at three different dietary conditions for 11 weeks (Table 1).

121

122

## 123 2.1 Seawater temperature experiment

124 The seawater temperature experiment started on 27 March 2011 and ended on 21 July 2011. Prior  
125 to the start of the experiment the animals were marked with calcein. The staining leaves a clear  
126 fluorescent marker in the shells that can be used to identify which shell material has formed prior  
127 to and during the experiment. Initially, the animals were kept at  $10.3 \pm 0.2$  °C for 48 days. Then,  
128 they were briefly removed from the tanks and marked again. Subsequently, the clams were cultured  
129 for 69 more days at  $15.0 \pm 0.3$  °C. Ambient seawater was pumped from the adjacent Damariscotta  
130 River estuary and adjusted to desired temperature. The salinity was measured with a Hydrolab®  
131 MiniSonde. It ranged between  $30.2 \pm 0.7$  and  $30.7 \pm 0.7$ , in the two experimental phases,  
132 respectively. During the entire culture period, all clams were exposed to ambient food conditions.  
133 At the end of the experiment the soft tissues were removed.

134

135

## 136 2.2 Food experiment



137 The food experiment was carried out from 9 February 2015 to 29 April 2015. The animals were  
138 placed in aquaria inside a climate room at 9 °C. Water temperature in the tanks ranged between 8  
139 and 10 °C. Water salinity was measured by using an ENDECO 102 refractometer and ranged  
140 between 29.6 and 29.9 ± 0.1 in each aquarium. The 15-liter tanks were constantly supplied with  
141 aerated water from the Wadden Sea. The clams were acclimated for three weeks before the start of  
142 the experiment. Three dietary regimes were chosen. One treatment consisted of feeding the animals  
143 with Microalgae Mix (food type 1), a ready-made solution of four marine microalgae (25 %  
144 *Isochrysis*, 25 % *Tetraselmis*, 25 % *Thalassiosira*, 25 % *Nannochloropsis*) with a particle size  
145 range of 2 - 30 µm. A second treatment was based on PhytoMaxx (food type 2), a solution of living  
146 *Nannochloropsis* algae with 2 - 5 µm size range. A third treatment served as control, i.e., the  
147 animals were not fed with any additional food. In treatments with food type 1 and 2, microalgae  
148 were provided at the constant optimum concentration of 20 × 10<sup>6</sup> cells/liter (Winter, 1969). A  
149 dispenser equipped with a timer was used to distribute the food five times per day. At the end of  
150 the experiment the soft tissues were removed. A distinct dark line in the shells indicated the  
151 transposition to the NIOZ aquaria and the associated stress. This line marks the beginning of the  
152 tank experiment.

153

154

### 155 2.3 Sample preparation

156 The right valve of each specimen was cut into two 1.5 millimeter-thick sections along the axis of  
157 maximum growth. For this purpose, a low speed precision saw (Buehler Isomet 1000) was used.  
158 Given the small size and fragility of the juvenile shells used in the food experiment, the valves  
159 were fully embedded in a block of Struers EpoFix (epoxy) and air-dried overnight prior the



160 sectioning. Sections of the clams used in the temperature experiment were embedded in epoxy after  
161 the cutting. All samples were ground using a Buehler Metaserv 2000 machine equipped with  
162 Buehler silicon carbide papers of different grit sizes (P320, P600, P1200, P2500). In addition, the  
163 samples were manually ground with Buehler P4000 grit paper and polished with a Buehler diamond  
164 polycrystalline suspension (3  $\mu\text{m}$ ). Sample surfaces were rinsed in demineralized water and air-  
165 dried. In the samples of the temperature experiment, the calcein marks were located under a  
166 fluorescence light microscope (Zeiss Axio Imager.A1m microscope equipped with a Zeiss  
167 HBO100 mercury lamp and filter set 38: excitation wavelength, ca. 450 - 500 nm; emission  
168 wavelength, ca. 500 - 550 nm).

169

170

#### 171 2.4 A. *islandica* shell organization

172 The shell of *A. islandica* consists of pure aragonite and it is divided in two major layers, an outer  
173 (OSL) and the inner shell layer (ISL). The OSL is further subdivided in outer (oOSL) and inner  
174 portion (iOSL) (Schöne, 2013). These layers are characterized by specific microstructures (Ropes  
175 et al., 1984). The oOSL largely consists of homogenous microstructure with a bulky and granular  
176 aspect (Schöne et al., 2013). The iOSL and ISL are largely composed of crossed-lamellar to cross-  
177 acicular microstructures (Dunca et al., 2009). The present study focuses on ventral margin of the  
178 shells. Analyses were carried out exclusively in the OSL.

179 Similar to other mollusks, the shell of *A. islandica* contains pigment polyenes which are  
180 obviously visible when using CRM (Hedegaard et al., 2006). Polyenes are organic compounds  
181 containing single (C-C) and double (C=C) carbon-carbon bonds forming a polyenic chain. Their





182 distribution across the shell is not homogenous. The pigments are abundant in the oOSL whereas  
183 they become scarce in the iOSL (Stemmer and Nehrke, 2014).

184

185

## 186 2.5 Confocal Raman microscopy and image processing

187 Shells were mapped with a WITec alpha 300 R (WITec GmbH, Germany) confocal Raman  
188 microscope. Scans of  $50 \times 50 \mu\text{m}$ ,  $100 \times 50 \mu\text{m}$  and  $150 \times 50 \mu\text{m}$  were performed using a  
189 piezoelectric scanner table. All Raman measurements were carried out using a 488 nm diode laser.  
190 A spectrometer (UHTS 300, WITec, Germany) was used with a  $600 \text{ mm}^{-1}$  grating, a 500 nm blaze  
191 and an integration time of 0.03 s. On each sample two to six scans were made, depending of the  
192 thickness of the shell. For instance, in juvenile shells (food experiment), two scans of each sample  
193 were made. On larger shells used in the temperature experiment, six maps were completed, i.e.,  
194 two maps in the oOSL, two in the middle of the iOSL and two in the inner portion of the iOSL.  
195 Each scan contained between 40,000 and 120,000 data points, depending on the map size. The  
196 spatial resolution equaled 250 nm. Half of the maps were performed on the shell portion formed  
197 before the experiments. The other half were made on the shell portion formed under experimental  
198 conditions. In order to avoid areas affected by transplantation or marking stress, the scans were  
199 located far off the calcein and stress lines. Raman maps on food experiment shells were performed  
200  $300 \mu\text{m}$  away from the stress line. In the shells from the temperature experiment, the scans were  
201 made 1 mm away from the calcein mark.

202 Polarized Raman microscopy is known to provide comprehensive information about the  
203 crystallographic properties of the materials (Hopkins and Farrow, 1985). The aragonite spectrum



204 is characterized by two lattice modes (translation mode  $T_a$ ,  $152\text{cm}^{-1}$  and librational mode  $L_a$ ,  
205  $206\text{cm}^{-1}$ ) and the two internal modes (in-plane band  $\nu_4$ ,  $705\text{cm}^{-1}$  and symmetric stretch  $\nu_1$ ,  $1085\text{cm}^{-1}$ ).  
206 The ratio ( $R_{\nu_1/T_a}$ ) between peak intensities belonging to  $\nu_1$  and  $T_a$  is caused by different  
207 crystallographic orientations of the aragonitic units (Hopkins and Farrow, 1985; Nehrke and Nouet,  
208 2011). Within each scan,  $R_{\nu_1/T_a}$  was calculated for each data point. New spectral images were  
209 generated using WITecProject software (version 4.1, WITec GmbH, Germany). These images were  
210 then binarized by replacing all values above 2.5 with 1 and the others with 0. The orientation was  
211 quantified by calculating the area formed by pixels of value 1 over the total scan area. The imaging  
212 software Gwyddion (<http://gwyddion.net/> last checked: June 2016) was used for this purpose. The  
213 results were expressed in percentage.

214 The Raman scans of the food experiment shells were analyzed to investigate the pigment  
215 composition. Polyene peaks have definite positions in the spectrum according to the number of the  
216 C-C and C=C bonds of the chain, which are specific for certain types of pigments. The two major  
217 polyene peaks at  $\sim 1130$  ( $R_1$ ) and  $1520\text{ cm}^{-1}$  ( $R_4$ ) were identified by using the “multipeak fitting 2”  
218 routine of IGOR Pro (version 7.00, WaveMetrics, USA). Their exact position was determined  
219 adopting a Gaussian fitting function (Fig. 2). The number of single ( $N_1$ ) and double carbon bonds  
220 ( $N_4$ ) was calculated by applying the equations by Schaffer et al. (1991):

$$221 \quad (1) \quad N_1 = 476 (R_1 - 1,082)$$

$$222 \quad (2) \quad N_4 = 830 (R_4 - 1,438)$$

223 Spectral images of the  $R_4$  band were used to locate the polyenes in the shell and measure the  
224 thickness of the pigmented layer. This analysis was conducted only on the shells of the food  
225 experiment. Given the larger size of the shells used in the temperature experiment, the spectral



226 maps were not sufficient for a correct localization of the pigmented layer boundaries and estimation  
227 of its thickness.

228 To quantify changes of the orientation of individual biomineral units of the juvenile shells  
229 (food experiment), the spectral maps were subdivided into two portions. The outermost shell  
230 portion (oOSL) was enriched in pigments whereas the iOSL showed a decrease in polyene content.

231

232

## 233 2.6 Scanning electron microscopy

234 After performing Raman measurements, the samples were prepared for SEM analysis. Each shell  
235 slab was ground with a Buehler Metaserv 2000 machine and Buehler silicon F2500 grit carbide  
236 paper. To reduce the impact of grinding on the sample surface of juvenile shells, extra grinding  
237 was done by hand. Then, the slabs were polished with a Buehler diamond polycrystalline  
238 suspension (3  $\mu\text{m}$ ). Afterward, shell surfaces were etched in 0.12 N HCl solution for 10 (food  
239 experiment samples) to 90 s (temperature experiment samples) and subsequently placed in 6 vol %  
240 NaClO solution for 30 min. After being rinsed in demineralized water, air-dried samples were  
241 sputter-coated with a 2 nm-thick platinum film by using a Low Vacuum Coater Leica EM ACE200.

242 A scanning electron microscope (LOT Quantum Design 2<sup>nd</sup> generation Phenom Pro desktop  
243 SEM) with backscattered electron detector and 10 kV accelerating voltage was used to analyze the  
244 shells. Images were taken at the same distances from the calcein and stress lines as in the case of  
245 the Raman measurements to assure comparability of the data.

246 In addition, stitched SEM images of the ventral margins were used to accurately determine  
247 the shell growth advance during the culturing experiments. Growth increment widths were



248 measured with the software Panopea (© Schöne and Peinl). Given the difference in duration of the  
249 two phases of the temperature experiment, the measurements were expressed as total growth and  
250 instantaneous growth rate (Fig. 3a + b). The latter was calculated using the following equation  
251 (Brey et al., 1990; Witbaard et al., 1997):

$$252 \quad (3) \text{ Instantaneous growth rate} = (\ln (y_t / y_0) / a)$$

253 where  $y_0$  represents the initial shell height,  $y_t$  is the final shell height and  $a$  is the duration of the  
254 experiment. In the case of the food experiment, only the total growth was calculated (Fig. 3c).

255

256

257

### 258 3. Results

#### 259 3.1 Effect of seawater temperature and diet on *A. islandica* shell growth

260 When exposed to a water temperature of 10 °C, the shells grew between 11.67 and 14.17 mm  
261 during a period of 48 days. During a period of 69 days at 15 °C, the growth ranged between 2.32  
262 and 5.77 mm (Fig. 3a). Instantaneous growth rate showed a decrease between the two experimental  
263 phases. At 10 and 15 °C, the average instantaneous growth per day was 0.0091 and 0.0013,  
264 respectively (Fig. 3b). The decrease in total growth and growth rate between the two temperatures  
265 was statistically significant ( $t$ -test,  $p < 0.01$ ).

266 During the food experiment, shells grew between 0.37 and 3.71 mm with large differences  
267 due to the different food types. Growth of specimens exposed to food type 1 ranged between 1.87  
268 to 3.71 mm, whereas those cultured with food type 2 grew between 0.55 to 0.96 mm. Both control



269 specimens added 0.37 mm of shell during the experimental phase (Fig. 3c). ANOVA and Tukey's  
270 HSD post hoc tests showed significant differences between specimens cultured with food type 1  
271 and 2 ( $p < 0.05$ ) and between food type 1 and control shells ( $p < 0.05$ ).

272

273

### 274 3.2 Effect of seawater temperature on *A. islandica* microstructure

275 At a water temperature of 10 °C, the area occupied by microstructural units oriented with  $R_{v1/Ta}$   
276 higher than 2.5 a.u. (= arbitrary units) ranged between 31.3 and 50.6 % in the oOSL and between  
277 21.3 and 33.5 % in the iOSL. When exposed to 15 °C, values ranged between 25.6 and 48.7 % and  
278 between 45.7 and 55.9 % in the oOSL and iOSL, respectively (Fig. 4). Whereas the slight difference  
279 of area with  $R_{v1/Ta} > 2.5$  in the oOSL was not significant between the two water temperatures ( $t$ -  
280 test,  $p = 0.62$ ), the area with  $R_{v1/Ta} > 2.5$  in the iOSL significantly increased at 15 °C ( $t$ -test,  $p =$   
281 0.02). Under the SEM, no difference was visible between units formed at 10 °C and 15 °C (Fig. 5).

282

283

### 284 3.3 Effect of food on *A. islandica* microstructure and pigments

285 In the shells cultured with food type 1, the area occupied by biomineral units oriented with  $R_{v1/Ta}$   
286 higher than 2.5 a.u. during the experiment ranged between 24.8 % (oOSL) and 43.0 % (iOSL). In  
287 the shell portion deposited before the experiment, the ratio varied between 19.4 % (oOSL) and 36.2  
288 % (iOSL). Although a trend was recognized, these variations were not statistically different ( $t$ -tests.  
289 OSL:  $p = 0.43$ ; ISL:  $p = 0.57$ ; Fig. 6a). On the contrary, in the clams exposed to food type 2, the



290 area occupied by units oriented with  $R_{v1/Ta} > 2.5$  ranged between 11.7 % (oOSL) and 20.4 %  
291 (iOSL). Before the experiment, the proportions were higher, i.e., 18.1% (oOSL) and 26.3% (iOSL)  
292 (Fig. 6b). As for the other treatment, the difference was not significant (*t*-tests. oOSL:  $p = 0.34$ ;  
293 iOSL:  $p = 0.28$ ). In the control shells grown with no extra food supply, the area with  $R_{v1/Ta} > 2.5$   
294 ranged between 24.6 % (oOSL) and 44.8 % (iOSL) during the experiment and 21.2 % (oOSL) and  
295 44.5 % (iOSL) before the experiment (Fig. 6c). Hence, no trend was visible and the two portions  
296 did not show significant differences (*t*-tests. oOSL:  $p = 0.59$ ; iOSL:  $p = 0.99$ ). As for the  
297 temperature experiment, under the SEM, the microstructure of the shells from the food experiment  
298 did not show any change (Fig. 7).

299 All treatments showed a slightly thicker pigmented layer formed during the experiment than  
300 during the acclimation phase (Fig. 8a). During the experiment, clams cultured with food type 1  
301 showed, on average, a thickening by 6.4 %. In the food type 2 specimens, the layer thickness  
302 increased by 9.9 %. Control shells showed an increase of 10.4 % (Fig. 8b). However, none of these  
303 differences was statistically significant (*t*-test. Food type 1:  $p = 0.43$ ; Food type 2:  $p = 0.39$ ; Control:  
304  $p = 0.10$ ). According to the position of the polyene peaks, the number of single carbon bonds in the  
305 pigment chain did not change between the acclimation and experimental phase ( $N_1 = 10.1 \pm 1.3$   
306 and  $N_1 = 10.0 \pm 0.9$ , respectively). Likely, no significant variation was observed in the number of  
307 double carbon bonds ( $N_4 = 10.5 \pm 0.2$  and  $N_4 = 10.4 \pm 0.3$ , respectively; Table 2).

308

309

310

311



## 312 4. Discussion

313 According to the results, variations of both food type and water temperature can influence the shell  
314 production rate of *A. islandica*. However, the shell microstructure and pigmentation react  
315 differently to these two environmental variables. Whereas changes of the dietary conditions do not  
316 affect the shell architecture and pigment composition, the crystallographic orientation of the  
317 biomineral units responds to seawater temperature fluctuations.

318

319

### 320 4.1 Environmental influence on shell microstructure

321 The environmental conditions experienced by mollusks during the process of biomineralization  
322 appear to influence shell organization (Carter, 1980). Among the different environmental variables,  
323 water temperature is the most studied driving force of structural changes of the shell. For instance,  
324 shell mineralogy can vary depending on water temperature (Carter, 1980). According to the thermal  
325 potentiation hypothesis, nucleation and growth of calcitic structural units is favored at low  
326 temperatures by kinetic factors (Carter et al., 1998). As a consequence, bivalve species living in  
327 cold water environments exhibit additional or thicker calcitic layers compared to the corresponding  
328 species from warm waters (Lowenstam, 1954; Taylor and Kennedy, 1969). Changes in the calcium  
329 carbonate polymorph also affect the type of microstructures (Milano et al., 2016). However,  
330 architectural variations often occur without mineralogical impact (Carter, 1980).

331 The present results indicate that temperature induces a change in the crystallographic  
332 orientation of the biomineral units of *A. islandica*. Although water temperature was previously  
333 shown to have an impact on microstructure formation, the attention has been mainly addressed to



334 the effects on the morphometric characteristics (e.g. size and shape) or on the type of  
335 microstructure. Milano et al. (2015) demonstrated that size and elongation of prismatic structural  
336 units of *Cerastoderma edule* were positively correlated to seawater temperature variation  
337 throughout the growing season. Likely, low temperatures induced the formation of small nacre  
338 tablets in *Geukensia demissa* (Lutz, 1984). Seasonal changes of the microstructural type were  
339 reported in the freshwater bivalve *Corbicula fluminea* (Prezant and Tan Tiu, 1986; Tan Tiu and  
340 Prezant, 1989). During the warm months, crossed acicular structure was produced, whereas simple  
341 crossed-lamellae were formed during the winter period. So far, variations of the crystallographic  
342 properties of bivalve biominerals have been exclusively investigated as a response to hypercapnic  
343 (acidified) conditions. *Mytilus galloprovincialis* and *Mytilus edulis* showed a significant change in  
344 the orientation of the prisms forming shell calcitic layer when subjected to hypercapnia (Hahn et  
345 al., 2012; Fitzer et al., 2014). Altered crystallographic organization may derive from the animal  
346 exposure to suboptimal conditions. These findings together with the present results suggest that  
347 thermal- and hypercapnic-induced stress are likely to affect the ability of the bivalves to preserve  
348 the orientation of their microstructural units (Fitzer et al., 2015).

349 Different food sources do not significantly influence the orientation of the biomineral units  
350 or the composition and distribution of pigments in shells of *A. islandica*. In previous studies, the  
351 relationship between microstructure and diet was virtually overlooked resulting in a lack of data in  
352 the literature. As suggested by Hedegaard et al., (2006), however, the type of polyenes is influenced  
353 by food. The ingestion of pigment-enriched microalgae potentially leads to an accumulation of  
354 pigments in mollusk tissues and the shell (Soldatov et al., 2013). On the other hand, it has been  
355 argued that polyenes do not generate from food sources like other pigments (i.e., carotenoids), but  
356 they are locally synthesized (Karampelas et al., 2009). In accordance to Stemmer and Nehrke  
357 (2014), the results presented here support the view that the specific diets on which the animals rely





358 on do not influence shell pigment composition. The chemical characteristics of the polyenes are  
359 likely to be specie-specific and independent from the habitats.

360

361

#### 362 4.2 Confocal Raman microscopy as tool for microstructural analysis

363 From a methodological perspective, the present study represents an innovative approach in  
364 the investigation of shell microstructural organization. Electron backscatter diffraction (EBSD) has  
365 been previously used to determine the crystallographic orientation of gastropod (Fryda et al., 2009;  
366 Pérez-Huerta et al., 2011) and bivalve microstructural units (Checa et al., 2006; Frenzel et al., 2012;  
367 Karney et al., 2012). Whereas, CRM on mollusk shells is generally applied within studies on  
368 taphonomic mineralogical alteration and pigment identification (Stemmer and Nehrke, 2014;  
369 Beierlein et al., 2015). Both techniques provide considerably high spatially resolved analysis up to  
370 250 nm, allowing the identification of individual structural units at  $\mu\text{m}$ - and  $\text{nm}$ -scale (Cusack et  
371 al., 2008; Karney et al., 2012). CRM offers important advantages supporting a broader application  
372 of this methodology in the biomineralization research field. For instance, samples do not require  
373 any pre-treatment. Unlike EBSD, there is no need of preparing thin-sections ( $\sim 150 \mu\text{m}$  thick) or  
374 etching the shell surface (Griesshaber et al., 2010; Hahn et al., 2012). Therefore, further structural  
375 and geochemical analyses can be easily performed on the same sections (Nehrke et al., 2012). In  
376 addition, the size of CRM scans can be remarkably large ( $\sim 7\text{-}8 \text{ mm}^2$ ) without compromising the  
377 achievable resolution. By overlapping adjacent scans, it is possible to produce stitched scans  
378 allowing to further increase the region of interest on the shell surface.



379 SEM has previously been demonstrated to provide a convenient approach for the  
380 identification of individual structural units and the quantification of potential changes occurring  
381 within them (Milano et al., 2015, 2016b). However, SEM exclusively provides information about  
382 the morphometric characteristics of the microstructural units. As highlighted by the present study,  
383 to achieve an exhaustive examination, it is suggested to combine SEM with techniques assessing  
384 crystallographic properties of the biomaterials. For instance, our results show that the effect of  
385 water temperature is detectable in crystallographic orientation but not in morphometric features of  
386 the biomineral units.

387

### 388 4.3 Environmental influence on shell growth

389 Numerous previous studies demonstrated that growth rate of *A. islandica* - and many other bivalves  
390 - is linked to environmental variables (e.g., Witbaard et al., 1997, 1999; Schöne et al., 2004; Butler  
391 et al., 2010; Mette et al., 2016). However, the relative importance of the main factors, temperature  
392 and food supply/quality driving shell formation are still not well understood. Positive correlations  
393 between shell growth and water temperature have been identified (i.e., Schöne et al., 2005;  
394 Wanamaker et al., 2009; Marali et al., 2015), but the relationship between shell growth and  
395 environment is more complex (Marchitto et al., 2010; Stott et al., 2010; Schöne et al., 2013) and  
396 likely dependent on the synergic effect of food availability and water temperature (Butler et al.,  
397 2013; Lohmann and Schöne, 2013; Mette et al., 2016). Tank experiments were run in order to  
398 precisely identify the role of these two parameters of shell growth of *A. islandica* (Witbaard et al.,  
399 1997; Hiebenthal et al., 2012). A tenfold increase in instantaneous growth rate was observed  
400 between 1 and 12 °C, with the greatest variation occurring below 6 °C (Witbaard et al., 1997). On  
401 the contrary, a temperature increase between 4 and 16 °C was shown to produce a slowdown of



402 shell production (Hiebenthal et al., 2012). Our results are in agreement with the latter study and  
403 show a decrease in the instantaneous growth rate between 10 and 15 °C. High temperatures are  
404 often associated with an increase of free radical production (Abele et al., 2002). A large amount of  
405 energy then has to be allocated to limit oxidative cellular damage (Abele and Puntarulo, 2004).  
406 This translates into a higher accumulation of lipofuscin and slower shell production rate  
407 (Hiebenthal et al., 2013). The contrasting results of previous studies may be explained by individual  
408 differences in the tolerance toward temperature change (Marchitto et al., 2000).

409       Along with water temperature, food availability was also shown to influence *A. islandica*  
410 shell growth (Witbaard et al., 1997). At high algal cell densities, the siphon activity increased. This,  
411 in turn, was positively correlated to shell growth. Previous experiments used different combinations  
412 of algae such as *Isochrysis galbana* and *Dunaliella marina* (Witbaard et al., 1997), or  
413 *Nannochloropsis oculata*, *Phaeodactylum tricornutum* and *Chlorella* sp. (Hiebenthal et al., 2012)  
414 to grow the clams. However, there are still uncertainties about the composition of the primary food  
415 source for this species (Butler et al., 2010). Even though it is challenging to determine the preferred  
416 algal species, our results show that the use of a mixture of different algal species results in  
417 significantly faster shell growth than the used of just one algal species. In the natural environment,  
418 suspension feeders such as *A. islandica* preferentially ingest certain particle sizes (Rubenstein and  
419 Koehl, 1977; Jorgensen, 1996; Baker et al., 1998). The exposure to a limited algal size range, as in  
420 the case of food type 2, may affect shell growth. Furthermore, multispecific solutions contain a  
421 higher variability of biochemical components that better meet the nutritional requirements of the  
422 animal (Widdows, 1991). Our results are in good agreement with previous findings. For instance,  
423 it has been shown by Strömngren and Cary (1984) that *Mytilus edulis* shell growth increased as a  
424 result of a diet based on three different algal species. Furthermore, Epifanio (1979) tested the  
425 differences on the growth of *Crassostrea virginica* and *Mercenaria mercenaria* of a mixed diet



426 composed by *Isochrysis galbana* and *Thalassiosira pseudonana* and diets consisting of the single  
427 species. Faster growth was measured in the mixed diet treatment, indicating a synergic effect of  
428 the relative food composition (Epifanio, 1979). Likely, *Mytilus edulis* grew faster when reared with  
429 different types of mixed diets as opposed to monospecific diets (Galley et al., 2010).

430

431

432

## 433 5. Conclusions

434 *Arctica islandica* shell growth and biomineral orientation vary with changes in sewerage  
435 temperature. However, exposure to different food sources affect shell deposition rate but do not  
436 influence the organization of the biomineral units. Given the exclusive sensitivity to one  
437 environmental variable, the orientation of biomineral units may represent a promising new  
438 temperature proxy for paleoenvironmental reconstructions. However, additional studies are needed  
439 to further explore the subject. In particular, intra-individual variability influence on the results  
440 needs to be assessed. In the present study, a variation in the orientation between individuals was  
441 well visible and the risks associated have to be taken in account when considering further  
442 application of the possible proxy. Furthermore, the effect of other environmental variables such as  
443 salinity needs to be tested.

444 The innovative application of CRM for microstructural orientation and proxy development  
445 proved that the technique has large potential in this research direction. More studies are needed to  
446 validate its suitability in paleoclimatology experimental works.



447

448

## 449 Acknowledgements

450 The authors acknowledge the crew of the *F.V. Three of a Kind* for helping with the collection of  
451 the animals. Design and execution of the seawater temperature experiment were successfully  
452 realized thanks to the support of B. Beal, D. Gillikin, A. Lorrain and the Darling Marine Center  
453 scientific team. Funding for this study was kindly provided by the EU within the framework of the  
454 Marie Curie International Training Network ARAMACC (604802).

455

456

## 457 References

458 Abele, D., Heise, K., Pörtner, H. O. and Puntarulo, S.: Temperature-dependence of mitochondrial  
459 function and production of reactive oxygen species in the intertidal mud clam *Mya arenaria*,  
460 J. Exp. Biol., 205, 1831-1841, doi:10.1016/j.jeb.2011.04.007, 2012.

461 Abele, D. and Puntarulo, S.: Formation of reactive species and induction of antioxidant defence  
462 systems in polar and temperate marine invertebrates and fish, Comp. Biochem. Physiol. Part  
463 A, 138(4), 405-415, doi:10.1016/j.cbpa.2004.05.013, 2004.

464 Aizenberg, J., Weaver, J. C., Thanawala, M. S., Sundar, V. C., Morse, D. E. and Fratzl, P.: Skeleton  
465 of *Euplectella* sp.: structural hierarchy from the nanoscale to the macroscale, Science,  
466 309(5732), 275-278, doi:10.1126/science.1112255, 2005.



- 467 Andrus, C. F. T.: Shell midden sclerochronology, *Quat. Sci. Rev.*, 30(21-22), 2892-2905,  
468 doi:10.1016/j.quascirev.2011.07.016, 2011.
- 469 Baker, S. M., Levinton, J. S., Kurdziel, J. P. and Shumway, S. E.: Selective feeding and  
470 biodeposition by zebra mussels and their relation to changes in phytoplankton composition  
471 and seston load, *J. Shellfish Res.*, 17, 1207-1213, 1998.
- 472 Beierlein, L., Nehkre, G. and Brey, T.: Confocal Raman microscopy in sclerochronology: A  
473 powerful tool to visualize environmental information in recent and fossil biogenic archives,  
474 *Geochemistry Geophys. Geosystems*, 16, 325-335, doi:10.1002/2014GC005684.Key, 2015.
- 475 Beirne, E. C., Wanamaker, A. D. and Feindel, S. C.: Experimental validation of environmental  
476 controls on the  $\delta^{13}\text{C}$  of *Arctica islandica* (ocean quahog) shell carbonate, *Geochim.*  
477 *Cosmochim. Acta*, 84, 395-409, doi:10.1016/j.gca.2012.01.021, 2012.
- 478 Berman, A., Hanson, J., Leiserowitz, L., Koetzle, T. F., Weiner, S. and Addadi, L.: Biological  
479 control of crystal texture: a widespread strategy for adapting crystal properties to function,  
480 *Science*, 259(5096), 776-779, doi:10.1126/science.259.5096.776, 1993.
- 481 Black, B. A., Gillespie, D. C., MacLellan, S. E. and Hand, C. M.: Establishing highly accurate  
482 production-age data using the tree-ring technique of crossdating: a case study for Pacific  
483 geoduck (*Panopea abrupta*), *Can. J. Fish. Aquat. Sci.*, 65, 2572-2578, doi:10.1139/F08-158,  
484 2008.
- 485 Black, B. A., Griffin, D., van der Sleen, P., Wanamaker, A. D., Speer, J. H., Frank, D. C., Stahle,  
486 D. W., Pederson, N., Copenheaver, C. A., Trouet, V., Griffin, S. and Gillanders, B. M.: The  
487 value of crossdating to retain high-frequency variability, climate signals, and extreme events



488 in environmental proxies, *Glob. Chang. Biol.*, 22(7), 2582-2595, doi:10.1111/gcb.13256,  
489 2016.

490

491 Bøggild, O. B.: The shell structure of the mollusks, in *Det Kongelige Danske Videnskabernes*  
492 *Selskabs Skrifter, Natruvidenskabelig og Matematisk*, pp. 231-326, Afdeling., 1930.

493 Brey, T., Arntz, W. E., Pauly, D. and Rumohr, H.: *Arctica (Cyprina) islandica* in Kiel Bay (Western  
494 Baltic): growth, production and ecological significance, *J. Exp. Mar. Bio. Ecol.*, 136(3), 217-  
495 235, doi:10.1016/0022-0981(90)90162-6, 1990.

496 Butler, P. G., Richardson, C. A., Scourse, J. D., Wanamaker, A. D. Jr, Shammon, T. M. and  
497 Bennell, J. D.: Marine climate in the Irish Sea: analysis of a 489-year marine master  
498 chronology derived from growth increments in the shell of the clam *Arctica islandica*, *Quat.*  
499 *Sci. Rev.*, 29(13-14), 1614-1632, doi:10.1016/j.quascirev.2009.07.010, 2010.

500 Butler, P. G., Wanamaker, A. D. Jr, Scourse, J. D., Richardson, C. A. and Reynolds, D. J.:  
501 Variability of marine climate on the North Icelandic Shelf in a 1357-year proxy archive based  
502 on growth increments in the bivalve *Arctica islandica*, *Palaeogeogr. Palaeoclimatol.*  
503 *Palaeoecol.*, 373, 141-151, doi:10.1016/j.palaeo.2012.01.016, 2013.

504 Carter, J. G.: Environmental and biological controls of bivalve shell mineralogy and  
505 microstructure, in *Skeletal Growth of Aquatic Organisms: Biological Records of*  
506 *Environmental Change (Topics in Geobiology)*, edited by D. C. Rhoads and R. A. Lutz, pp.  
507 69-113, Plenum, N. Y, 1980.



- 508 Carter, J. G. and Clark, G. R. I.: Classification and phylogenetic significance of molluscan shell  
509 microstructure, in Mollusks, Notes for a Short Course, edited by T. W. Broadhead, pp. 50-  
510 71., 1985.
- 511 Carter, J. G., Barrera, E. and Tevesz, M. T. S.: Thermal potentiation and mineralogical evolution  
512 in the Bivalvia (Mollusca), *J. Paleontol.*, 72(6), 991-1010, 1998.
- 513 Carter, J. G., Harries, P. J., Malchus, N., Sartori, A. F., Anderson, L. C., Bieler, R., Bogan, A. E.,  
514 Coan, E. V., Cope, J. C. W., Cragg, S. M., Garcia-March, J. R., Hylleberg, J., Kelley, P.,  
515 Kleemann, K., Kriz, J., McRoberts, C., Mikkelsen, P. M., Pojeta, J. J., Temkin, I., Yancey,  
516 T. and Zieritz, A.: Illustrated glossary of the bivalvia, *Treatise Online*, 1(48), 2012.
- 517 Checa, A. G., Okamoto, T. and Ramírez, J.: Organization pattern of nacre in Pteriidae (Bivalvia:  
518 Mollusca) explained by crystal competition., *Proc. Biol. Sci.*, 273(1592), 1329-37,  
519 doi:10.1098/rspb.2005.3460, 2006.
- 520 Currey, J. D.: The design of mineralised hard tissues for their mechanical functions, *J. Exp. Biol.*,  
521 202, 3285-3294, 1999.
- 522 Cusack, M., Parkinson, D., Freer, A., Pérez-Huerta, A., Fallick, A. E. and Curry, G. B.: Oxygen  
523 isotope composition in *Modiolus modiolus* aragonite in the context of biological and  
524 crystallographic control, *Mineral. Mag.*, 72(2), 569-577,  
525 doi:10.1180/minmag.2008.072.2.569, 2008.
- 526 Dauphin, Y., Cuif, J. P., Doucet, J., Salomé, M., Susini, J. and Willams, C. T.: In situ chemical  
527 speciation of sulfur in calcitic biominerals and the simple prism concept, *J. Struct. Biol.*,  
528 142(2), 272-280, doi:10.1016/S1047-8477(03)00054-6, 2003.





- 529 Deith, M. R.: The composition of tidally deposited growth lines in the shell of the edible cockle,  
530 *Cerastoderma edule*, J. Mar. Biol. Assoc. United Kingdom, 65(3), 573-581, 1985.
- 531 Dunca, E., Mutvei, H., Göransson, P., Mörth, C.-M., Schöne, B. R., Whitehouse, M. J., Elfman,  
532 M. and Baden, S. P.: Using ocean quahog (*Arctica islandica*) shells to reconstruct  
533 palaeoenvironment in Öresund, Kattegat and Skagerrak, Sweden, Int. J. Earth Sci., 98(1), 3-  
534 17, doi:10.1007/s00531-008-0348-6, 2009.
- 535 Epifanio, C. E.: Growth in bivalve molluscs: nutritional effects of two or more species of algae in  
536 diets fed to the American oyster *Crassostrea virginica* (Gmelin) and the hard clam  
537 *Mercenaria mercenaria* (L.), Aquaculture, 18, 1-12, 1979.
- 538 Epstein, S., Buchbaum, R., Lowenstam, H. A. and Urey, H. C.: Revised carbonate-water isotopic  
539 temperature scale. Bull. Geol. Soc. Am., 64, 1315-1326, 1953.
- 540 Fitzer, S. C., Cusack, M., Phoenix, V. R. and Kamenos, N. A.: Ocean acidification reduces the  
541 crystallographic control in juvenile mussel shells, J. Struct. Biol., 188, 39-45,  
542 doi:10.1016/j.jsb.2014.08.007, 2014.
- 543 Fitzer, S. C., Zhu, W., Tanner, K. E., Phoenix, V. R., Nicholas, A. K. and Cusack, M.: Ocean  
544 acidification alters the material properties of *Mytilus edulis* shells, J. R. Soc. Interface,  
545 12(103), doi:10.1098/rsif.2014.1227Published, 2015.
- 546 Frenzel, M., Harrison, R. J. and Harper, E. M.: Nanostructure and crystallography of aberrant  
547 columnar vaterite in *Corbicula fluminea* (Mollusca), J. Struct. Biol., 178(1), 8-18,  
548 doi:10.1016/j.jsb.2012.02.005, 2012.



- 549 Fryda, J., Bandel, K. and Frydova, B.: Crystallographic texture of Late Triassic gastropod nacre:  
550 Evidence of long-term stability of the mechanism controlling its formation, *Bull. Geosci.*,  
551 84(4), 745-754, doi:10.3140/bull.geosci.1169, 2009.
- 552 Galley, T. H., Batista, F. M., Braithwaite, R., King, J. and Beaumont, A. R.: Optimisation of larval  
553 culture of the mussel *Mytilus edulis* (L.), *Aquac. Int.*, 18(3), 315-325, doi:10.1007/s10499-  
554 009-9245-7, 2010.
- 555 Gillikin, D. P., De Ridder, F., Ulens, H., Elskens, M., Keppens, E., Baeyens, W. and Dehairs, F.:  
556 Assessing the reproducibility and reliability of estuarine bivalve shells (*Saxidomus*  
557 *giganteus*) for sea surface temperature reconstruction: Implications for paleoclimate studies,  
558 *Palaeogeogr. Palaeoclimatol. Palaeoecol.*, 228(1-2), 70-85,  
559 doi:10.1016/j.palaeo.2005.03.047, 2005.
- 560 Gordon, J. and Carriker, M. R.: Growth lines in a bivalve mollusk: subdaily patterns and dissolution  
561 of the shell, *Science*, 202, 519-521, doi:10.1126/science.202.4367.519, 1978.
- 562 Griesshaber, E., Neuser, R. D. and Schmahl, W. W.: The application of EBSD analysis to  
563 biomaterials: microstructural and crystallographic texture variations in marine carbonate  
564 shells, *Semin Soc Esp Miner.*, 7, 22-34, 2010.
- 565 Grossman, E. L. and Ku, T.: Oxygen and carbon isotope fractionation in biogenic aragonite:  
566 Temperature effects, *Chem. Geol.*, 59, 59-74, 1986.
- 567 Hahn, S., Rodolfo-Metalpa, R., Griesshaber, E., Schmahl, W. W., Buhl, D., Hall-Spencer, J. M.,  
568 Baggini, C., Fehr, K. T. and Immenhauser, A.: Marine bivalve shell geochemistry and  
569 ultrastructure from modern low pH environments: environmental effect versus experimental  
570 bias, *Biogeosciences*, 9, 1897-1914, doi:10.5194/bg-9-1897-2012, 2012.



- 571 Hedegaard, C., Bardeau, J. F. and Chateigner, D.: Molluscan shell pigments: An in situ resonance  
572 Raman study, *J. Molluscan Stud.*, 72(2), 157-162, doi:10.1093/mollus/eyi062, 2006.
- 573 Hiebenthal, C., Philipp, E., Eisenhauer, A. and Wahl, M.: Interactive effects of temperature and  
574 salinity on shell formation and general condition in Baltic Sea *Mytilus edulis* and *Arctica*  
575 *islandica*, *Aquat. Biol.*, 14(3), 289-298, doi:10.3354/ab00405, 2012.
- 576 Hiebenthal, C., Philipp, E. E. R., Eisenhauer, A. and Wahl, M.: Effects of seawater  $p\text{CO}_2$  and  
577 temperature on shell growth, shell stability, condition and cellular stress of Western Baltic  
578 Sea *Mytilus edulis* (L.) and *Arctica islandica* (L.), *Mar. Biol.*, 160, 2073-2087,  
579 doi:10.1007/s00227-012-2080-9, 2013.
- 580 Hopkins, J. B. and Farrow, L. A.: Raman microprobe determination of local crystal orientation, *J.*  
581 *Appl. Phys.*, 59(4), 1103-1110, doi:10.1063/1.336547, 1985.
- 582 Jones, D. S.: Sclerochronology: Shell record of the molluscan shell, *Am. Sci.*, 71(4), 384-391,  
583 1983.
- 584 Jorgensen, C. B.: Bivalve filter feeding revisited, *Mar. Ecol. Prog. Ser.*, 142(1-3), 287-302,  
585 doi:10.3354/meps142287, 1996.
- 586 Karampelas, S., Fritsch, E., Mevellec, J. Y., Sklavounos, S. and Soldatos, T.: Role of polyenes in  
587 the coloration of cultured freshwater pearls, *Eur. J. Mineral.*, 21(1), 85-97, doi:10.1127/0935-  
588 1221/2009/0021-1897, 2009.
- 589 Karney, G. B., Butler, P. G., Speller, S., Scourse, J. D., Richardson, C. A., Schröder, M., Hughes,  
590 G. M., Czernuszka, J. T. and Grovenor, C. R. M.: Characterizing the microstructure of  
591 *Arctica islandica* shells using NanoSIMS and EBSD, *Geochemistry, Geophys. Geosystems*,  
592 13(4), doi:10.1029/2011GC003961, 2012.



- 593 Lohmann, G. and Schöne, B. R.: Climate signatures on decadal to interdecadal time scales as  
594 obtained from mollusk shells (*Arctica islandica*) from Iceland, *Palaeogeogr. Palaeoclimatol.*  
595 *Palaeoecol.*, 373, 152-162, doi:10.1016/j.palaeo.2012.08.006, 2013.
- 596 Lowenstam, H. A.: Factors affecting the aragonite: calcite ratios in carbonate-secreting marine  
597 organisms, *J. Geol.*, 62(3), 284-322, 1954.
- 598 Lowenstam, H. A. and Weiner, S.: *On biomineralization*, Oxford University Press, New York.,  
599 1989, pp.324.
- 600 Lutz, R. A.: Paleocological implications of environmentally-controlled variation in molluscan  
601 shell microstructure, *Geobios*, 17, 93-99, doi:10.1016/S0016-6995(84)80161-8, 1984.
- 602 Marali, S. and Schöne, B. R.: Oceanographic control on shell growth of *Arctica islandica*  
603 (*Bivalvia*) in surface waters of Northeast Iceland - Implications for paleoclimate  
604 reconstructions, *Palaeogeogr. Palaeoclimatol. Palaeoecol.*, 420, 138-149,  
605 doi:10.1016/j.palaeo.2014.12.016, 2015.
- 606 Marchitto, T. M., Jones, G. A., Goodfriend, G. A. and Weidman, C. R.: Precise temporal  
607 correlation of Holocene mollusk shells using sclerochronology, *Quat. Res.*, 53, 236-246,  
608 doi:10.1006/qres.1999.2107, 2000.
- 609 Merkel, C., Griesshaber, E., Kelm, K., Neuser, R., Jordan, G., Logan, A., Mader, W. and Schmahl,  
610 W. W.: Micromechanical properties and structural characterization of modern inarticulated  
611 brachiopod shells, *J. Geophys. Res.*, 112(G02008), doi:10.1029/2006JG000253, 2007.
- 612 Mette, M. J., Wanamaker, A. D., Carroll, M. L., Ambrose, W. G. and Retelle, M. J.: Linking large-  
613 scale climate variability with *Arctica islandica* shell growth and geochemistry in northern  
614 Norway, *Limnol. Oceanogr.*, 61(2), 748-764, doi:10.1002/lno.10252, 2016.



- 615 Milano, S., Schöne, B. R. and Witbaard, R.: Changes of shell microstructural characteristics of  
616 *Cerastoderma edule* (Bivalvia) - A novel proxy for water temperature, *Palaeogeogr.*  
617 *Palaeoclimatol. Palaeoecol.*, doi:10.1016/j.palaeo.2015.09.051, 2015.
- 618 Milano, S., Prendergast, A. L. and Schöne, B. R.: Effects of cooking on mollusk shell structure and  
619 chemistry: Implications for archeology and paleoenvironmental reconstruction, *J. Archaeol.*  
620 *Sci. Reports*, 7, 14-26, doi: 10.1016/j.jasrep.2016.03.045, 2016.
- 621 Milano, S., Schöne, B. R., Wang, S. and Müller, W. E.: Impact of high  $p\text{CO}_2$  on shell structure of  
622 the bivalve *Cerastoderma edule*, *Mar. Environ. Res.*, 119, 144-155,  
623 doi:10.1016/j.marenvres.2016.06.002, 2016b.
- 624 Mook, W.: Paleotemperatures and chlorinities from stable carbon and oxygen isotopes in shell  
625 carbonate, *Palaeogeogr. Palaeoclimatol. Palaeoecol.*, 9(4), 245-263, doi:10.1016/0031-  
626 0182(71)90002-2, 1971.
- 627 Nehrke, G. and Nouet, J.: Confocal Raman microscope mapping as a tool to describe different  
628 mineral and organic phases at high spatial resolution within marine biogenic carbonates: case  
629 study on *Nerita undata* (Gastropoda, Neritopsina), *Biogeosciences*, 8, 3761-3769,  
630 doi:10.5194/bg-8-3761-2011, 2011.
- 631 Nishida, K., Ishimura, T., Suzuki, A. and Sasaki, T.: Seasonal changes in the shell microstructure  
632 of the bloody clam, *Scapharca broughtonii* (Mollusca: Bivalvia: Arcidae), *Palaeogeogr.*  
633 *Palaeoclimatol. Palaeoecol.*, 363-364, 99-108, doi:10.1016/j.palaeo.2012.08.017, 2012.
- 634 Nudelman, F., Gotliv, B. A., Addadi, L. and Weiner, S.: Mollusk shell formation: mapping the  
635 distribution of organic matrix components underlying a single aragonitic tablet in nacre, *J.*  
636 *Struct. Biol.*, 153, 176-187, doi:10.1016/j.jsb.2005.09.009, 2006.



- 637 Pérez-Huerta, A., Dauphin, Y., Cuif, J. P. and Cusack, M.: High resolution electron backscatter  
638 diffraction (EBSD) data from calcite biominerals in recent gastropod shells, *Micron*, 42(3),  
639 246-51, doi:10.1016/j.micron.2010.11.003, 2011.
- 640 Pérez-Huerta, A., Etayo-Cadavid, M. F., Andrus, C. F. T., Jeffries, T. E., Watkins, C., Street, S. C.  
641 and Sandweiss, D. H.: El Niño impact on mollusk biomineralization-implications for trace  
642 element proxy reconstructions and the paleo-archeological record. *PLoS One*, 8(2), e54274,  
643 doi:10.1371/journal.pone.0054274, 2013.
- 644 Prezant, R. S. and Tan Tiu, A.: Spiral crossed-lamellar shell growth in *Corbicula* (Mollusca:  
645 Bivalvia), *Trans. Am. Microsc. Soc.*, 105(4), 338-347, 1986.
- 646 Richardson, C. A.: Molluscs as archives of environmental change, *Oceanogr. Mar. Biol. an Annu.*  
647 *Rev.*, 39, 103-164, 2001.
- 648 Rodríguez-Navarro, A. B., CabraldeMelo, C., Batista, N., Morimoto, N., Alvarez-Lloret, P.,  
649 Ortega-Huertas, M., Fuenzalida, V. M., Arias, J. I., Wiff, J. P. and Arias, J. L.: Microstructure  
650 and crystallographic-texture of giant barnacle (*Austromegabalanus psittacus*) shell, *J. Struct.*  
651 *Biol.*, 156, 355-362, doi:10.1016/j.jsb.2006.04.009, 2006.
- 652 Ropes, J. W., Jones, D. S., Murawski, S. A., Serchuk, F. M. and Jearld, A.: Documentation of  
653 annual growth lines in ocean quahogs, *Artica islandica* Linne, *Fish. Bull.*, 82(1), 1-19, 1984.
- 654 Rubenstein, D. I. and Koehl, M. A. R.: The mechanisms of filter feeding: some theoretical  
655 considerations, *Am. Nat.*, 111, 981-994, 1977.
- 656 Schaffer, H. E., Chance, R. R., Silbey, R. J., Knoll, K. and Schrock, R. R.: Conjugation length  
657 dependence of Raman scattering in a series of linear polyenes: Implications for  
658 polyacetylene, *J. Chem. Phys.*, 94(6), 4161, doi:10.1063/1.460649, 1991.



- 659 Schöne, B. R.: The curse of physiology—challenges and opportunities in the interpretation of  
660 geochemical data from mollusk shells, *Geo-Marine Lett.*, 28, 269-285, doi:10.1007/s00367-  
661 008-0114-6, 2008.
- 662 Schöne, B. R.: *Arctica islandica* (Bivalvia): a unique paleoenvironmental archive of the northern  
663 North Atlantic Ocean, *Glob. Planet. Change*, 111, 199-225,  
664 doi:10.1016/j.gloplacha.2013.09.013, 2013.
- 665 Schöne, B. R. and Gillikin, D. P.: Unraveling environmental histories from skeletal diaries —  
666 Advances in sclerochronology, *Palaeogeogr. Palaeoclimatol. Palaeoecol.*, 373, 1-5,  
667 doi:10.1016/j.palaeo.2012.11.026, 2013.
- 668 Schöne, B. R. and Surge, D. M.: Part N , revised , volume 1 , chapter 14 : bivalve sclerochronology  
669 and geochemistry, *Treatise Online*, 1(46), 1-24, 2012.
- 670 Schöne, B. R., Freyre Castro, A. D., Fiebig, J., Houk, S. D., Oschmann, W. and Kröncke, I.: Sea  
671 surface water temperatures over the period 1884-1983 reconstructed from oxygen isotope  
672 ratios of a bivalve mollusk shell (*Arctica islandica*, southern North Sea), *Palaeogeogr.*  
673 *Palaeoclimatol. Palaeoecol.*, 212, 215-232, doi:10.1016/j.palaeo.2004.05.024, 2004.
- 674 Schöne, B. R., Fiebig, J., Pfeiffer, M., Gleß, R., Hickson, J., Johnson, A. L. A., Dreyer, W. and  
675 Oschmann, W.: Climate records from a bivalved Methuselah (*Arctica islandica*, Mollusca;  
676 Iceland), *Palaeogeogr. Palaeoclimatol. Palaeoecol.*, 228(1-2), 130-148,  
677 doi:10.1016/j.palaeo.2005.03.049, 2005.
- 678 Schöne, B. R., Radermacher, P., Zhang, Z. and Jacob, D. E.: Crystal fabrics and element impurities  
679 (Sr/Ca, Mg/Ca, and Ba/Ca) in shells of *Arctica islandica*—Implications for paleoclimate



- 680 reconstructions, *Palaeogeogr. Palaeoclimatol. Palaeoecol.*, 373, 50-59,  
681 doi:10.1016/j.palaeo.2011.05.013, 2013.
- 682 Soldatov, A. A., Gostyukhina, O. L., Borodina, A. V. and Golovina, I. V.: Qualitative composition  
683 of carotenoids, catalase and superoxide dismutase activities in tissues of bivalve mollusc  
684 *Anadara inaequalis* (Brugiere, 1789), *J. Evol. Biochem. Physiol.*, 49(4), 3889-398,  
685 doi:10.1134/S0022093013040026, 2013.
- 686 Stemmer, K. and Nehrke, G.: The distribution of polyenes in the shell of *Arctica islandica* from  
687 North Atlantic localities: a confocal Raman microscopy study, *J. Molluscan Stud.*, 80, 365-  
688 370, doi:10.1093/mollus/eyu033, 2014.
- 689 Stott, K. J., Austin, W. E. N., Sayer, M. D. J., Weidman, C. R., Cage, A. G. and Wilson, R. J. S.:  
690 The potential of *Arctica islandica* growth records to reconstruct coastal climate in north west  
691 Scotland, UK, *Quat. Sci. Rev.*, 29(13-14), 1602-1613, doi:10.1016/j.quascirev.2009.06.016,  
692 2010.
- 693 Strömgren, T. and Cary, C.: Growth in length of *Mytilus edulis* L. fed on different algal diets, *J.*  
694 *Exp. Mar. Bio. Ecol.*, 76(1), 23-34, doi:10.1016/0022-0981(84)90014-5, 1984.
- 695 Tan Tiu, A.: Temporal and spatial variation of shell microstructure of *Polymesoda caroliniana*  
696 (Bivalvia: Heterodonta), *Am. Malacol. Bull.*, 6(2), 199-206, 1988.
- 697 Tan Tiu, A. and Prezant, R. S.: Temporal variation in microstructure of the inner shell surface of  
698 *Corbicula fluminea* (Bivalvia: Heterodonta), *Am. Malacol. Bull.*, 7(1), 65-71, 1989.
- 699 Tan Tiu, A. and Prezant, R. S.: Shell microstructural responses of *Geukensia demissa granosissima*  
700 (Mollusca: Bivalvia) to continual submergence, *Am. Malacol. Bull.*, 5(2), 173-176, 1987.





701 Taylor, J.D. and Kennedy, W.J.: The shell structure and mineralogy of *Chama pellucida* inst  
702 electron microscope, *Veliger* 11: 391-398, 1969.

703 Thompson, I., Jones, D. S. and Dreibelbis, D.: Annual internal growth banding and life history of  
704 the ocean quahog *Arctica islandica* (Mollusca: Bivalvia), *Mar. Biol.*, 57, 25-34, 1980.

705 Wanamaker, A. D., Kreutz, K. J., Borns, H. W., Introne, D. S., Feindel, S., Funder, S., Rawson, P.  
706 D. and Barber, B. J.: Experimental determination of salinity, temperature, growth, and  
707 metabolic effects on shell isotope chemistry of *Mytilus edulis* collected from Maine and  
708 Greenland, *Paleoceanography*, 22(2), doi:10.1029/2006PA001352, 2007.

709 Wanamaker, A. D., Heinemeier, J., Scourse, J. D., Richardson, C. A., Butler, P. G., Eiríksson, J.  
710 and Knudsen, K. L.: Very long-lived mollusks confirm 17<sup>th</sup> century ad tephra-based  
711 radiocarbon reservoir ages for North Icelandic shelf waters, *Radiocarbon*, 50(3), 399-412,  
712 2008.

713 Wanamaker, A. D., Kreutz, K. J., Schöne, B. R., Maasch, K. A., Pershing, A. J., Borns, H. W.,  
714 Introne, D. S. and Feindel, S.: A late Holocene paleo-productivity record in the western Gulf  
715 of Maine, USA, inferred from growth histories of the long-lived ocean quahog (*Arctica*  
716 *islandica*), *Int. J. Earth Sci.*, 98(1), 19-29, doi:10.1007/s00531-008-0318-z, 2009.

717 Wanamaker, A. D., Hetzinger, S. and Halfar, J.: Reconstructing mid- to high-latitude marine  
718 climate and ocean variability using bivalves, coralline algae, and marine sediment cores from  
719 the Northern Hemisphere, *Palaeogeogr. Palaeoclimatol. Palaeoecol.*, 302(1), 1-9,  
720 doi:10.1016/j.palaeo.2010.12.024, 2011a.



- 721 Wanamaker, A. D., Butler, P. G., Scourse, J. D., Heinemeier, J., Eiríksson, J., Knudsen, K. L. and  
722 Richardson, C. A.: Surface changes in the North Atlantic meridional overturning circulation  
723 during the last millennium, *Paleoceanography*, 3, 237-252, doi:10.1038/ncomms1901, 2012.
- 724 Wanamaker, A. D., Mette, M. J. and Whitney, N.: The potential for the long- lived bivalve *Arctica*  
725 *islandica* to contribute to our understanding of past AMOC dynamics, *US CLIVAR Var.*, 14,  
726 13-19, 2016.
- 727 Wanamaker, A. D., Kreutz, K. J., Schöne, B. R. and Introne, D. S.: Gulf of Maine shells reveal  
728 changes in seawater temperature seasonality during the Medieval Climate Anomaly and the  
729 Little Ice Age, *Palaeogeogr. Palaeoclimatol. Palaeoecol.*, 302(1), 43-51,  
730 doi:10.1016/j.palaeo.2010.06.005, 2011b.
- 731 Weiner, S. and Addadi, L.: Acidic macromolecules of mineralized tissues: the controllers of crystal  
732 formation, *Trends Biochem. Sci.*, 16, 252-256, 1991.
- 733 Weiner, S. and Addadi, L.: Design strategies in mineralized biological materials, *J. Mater. Chem.*,  
734 7, 689-702, doi:10.1039/a604512j, 1997.
- 735 Widdows, J.: Physiological ecology of mussel larvae, *Aquaculture*, 94(2-3), 147-163,  
736 doi:10.1016/0044-8486(91)90115-N, 1991.
- 737 Winter, J. E.: Über den Einfluß der Nahrungskonzentration und anderer Faktoren auf  
738 Filtrierleistung und Nahrungsausnutzung der Muscheln *Arctica islandica* und *Modiolus*  
739 *modiolus*, *Mar. Biol.*, 4(2), 87-135, doi:10.1007/BF00347037, 1969.
- 740 Witbaard, R., Franken, R. and Visser, B.: Growth of juvenile *Arctica islandica* under experimental  
741 conditions, *Helgolaender Meeresuntersuchungen*, 51, 417-431, doi:10.1007/BF02908724,  
742 1997.

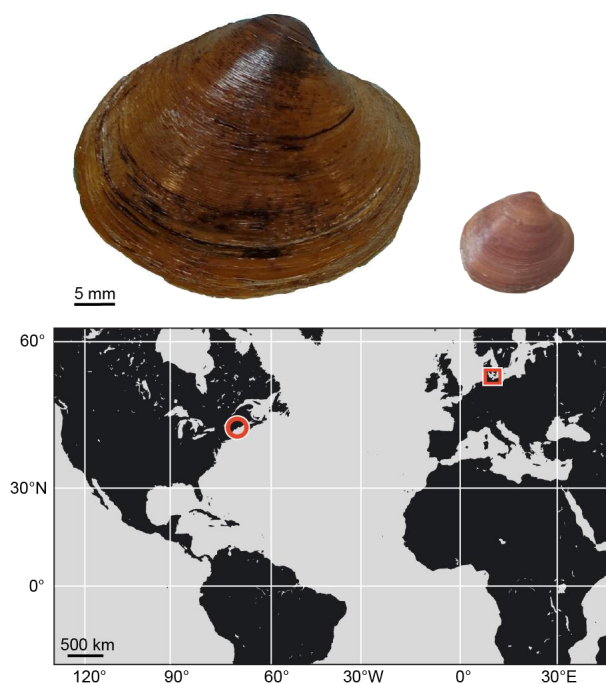


743 Witbaard, R., Duineveld, G. C. A. and de Wilde, P. A. W. J.: Geographical differences in growth  
744 rates of *Arctica islandica* (Mollusc: Bivalvia) from the North Sea and adjacent waters, J. Mar.  
745 Biol. Assoc. United Kingdom, 79, 907-915, 1999.

746

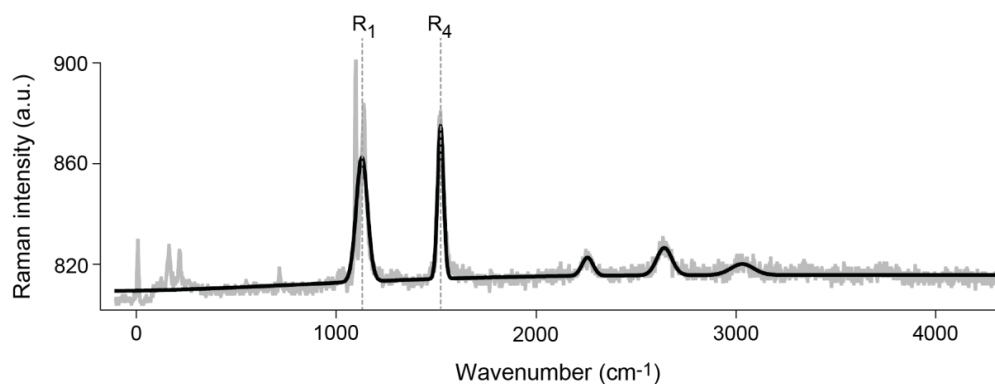
747

748 Figures and tables



749

750 **Fig. 1.** Shell of adult *Arctica islandica* used in the temperature experiment (left) and juvenile from the Baltic  
751 Sea used in the food experiment (right). The map indicates the localities where the two sets of shells were  
752 collected: Jonesport, Maine (circle) and Kiel Bay (square).

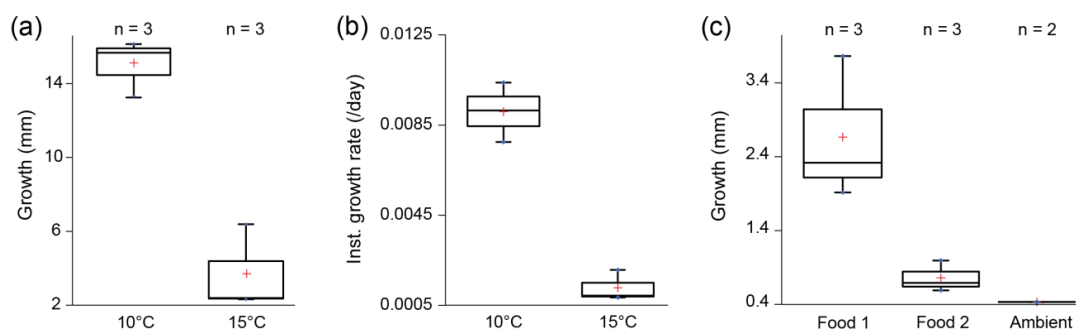


753

754 **Fig. 2.** Raman spectrum of *Arctica islandica* showing the typical aragonite peaks (grey line). The exact  
755 position of the polyene peaks R<sub>1</sub> and R<sub>4</sub> was determined by using a peak fitting routine based on a Gaussian  
756 function (black line).

757

758



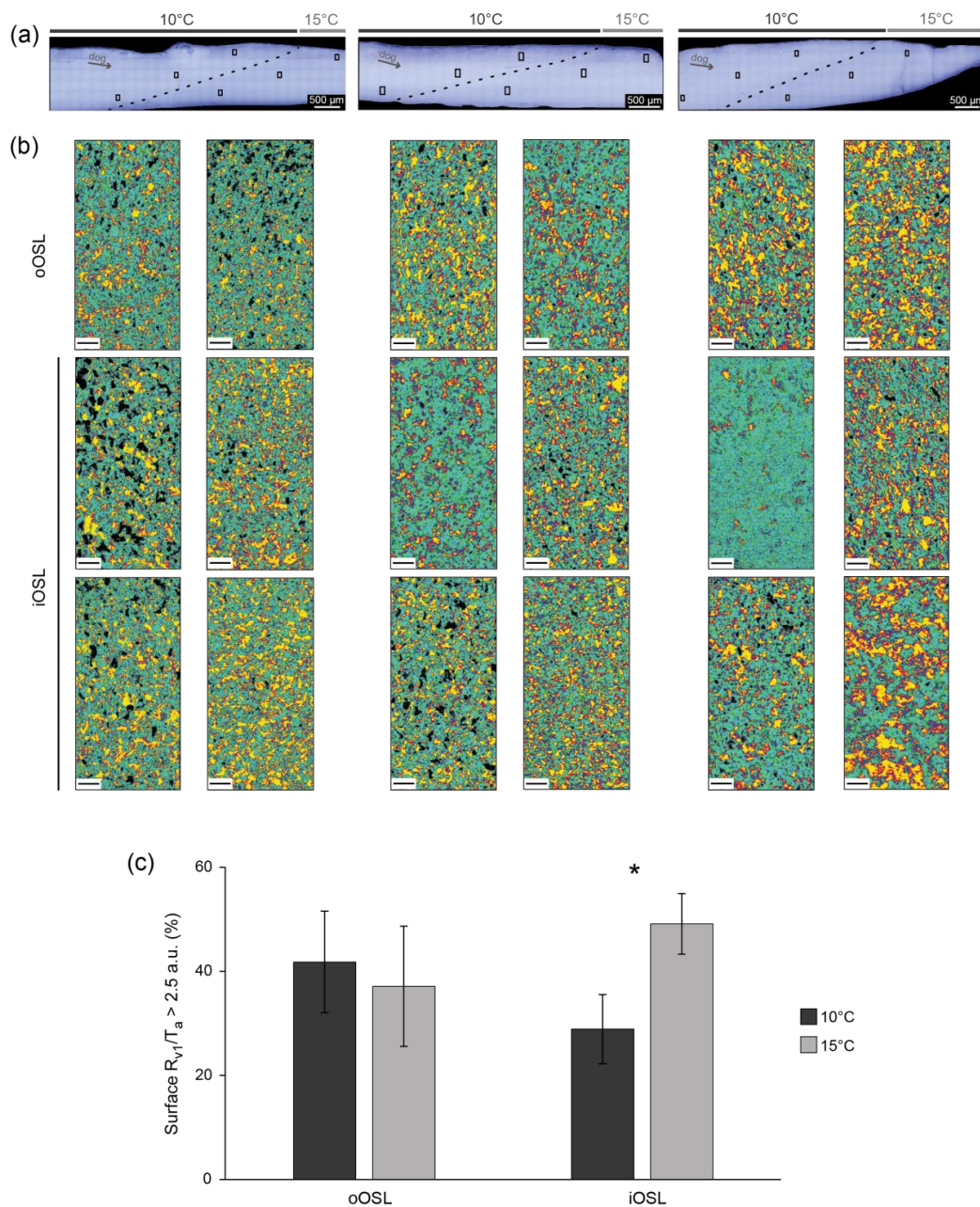
759

760 **Fig. 3.** *Arctica islandica* shell growth under controlled conditions. (a) Total growth and (b) instantaneous  
761 growth rate during the temperature experiment. (c) Total growth during the food experiment.

762

763

764



765

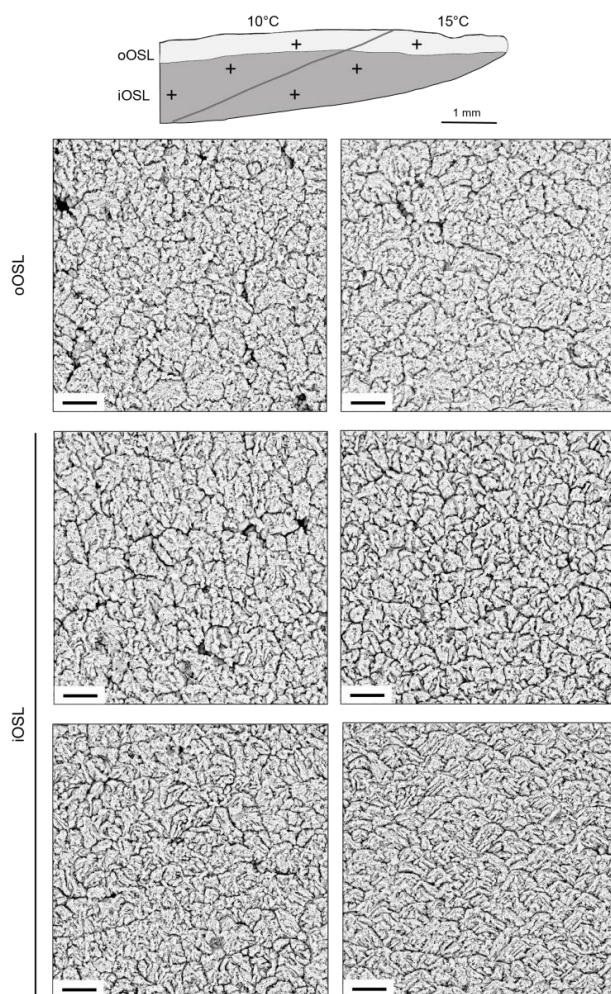
766 **Fig. 4.** Effect of temperature increase on biomineral orientation. (a) Position of the Raman maps of the three  
 767 specimens reared at 10 °C and 15 °C. Dotted lines indicate the location of the calcein marks. dog = direction  
 768 of growth. (b) Raman spectral maps of  $R_{v1/Ta}$ . Left images of each column represents shell portion formed



769 at 10 °C, right images represent shell portions formed at 15 °C. First row of pairs refers to oOSL, the other  
770 two represent the iOSL. Scale bars = 10 μm. (c) Proportions of biominerals with  $R_{v1/Ta} > 2.5$  a.u. with respect  
771 to the total map area. Asterisks indicate significant difference between the orientation of iOSL  
772 microstructures formed at 10 and 15°C ( $p < 0.05$ ).

773

774



775

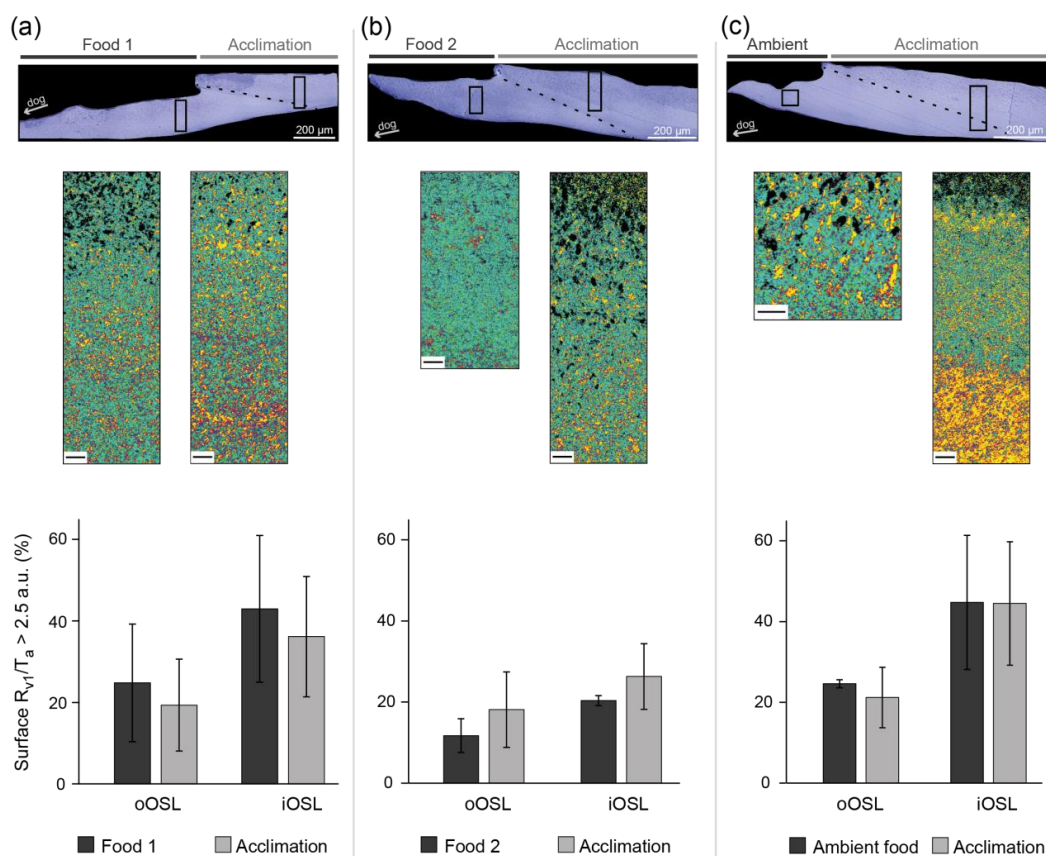
776



777 **Fig. 5.** SEM images of *Arctica islandica* shell microstructures formed at 10 °C (left column) and at 15 °C  
 778 (right column). The sketch indicates the position of the images 1 mm away from the calcein mark (grey  
 779 line). The first row of images refers to the oOSL, the other two row refers to the iOSL. Scale bars if not  
 780 otherwise indicated = 5 µm.

781

782



783

784 **Fig. 6.** Effect of different diets based on (a) food type 1, (b) food type 2 and (c) ambient food on biomineral  
 785 orientation. The optical microscope images indicate the position of the Raman scans. Dotted line marks the  
 786 start of the experiment. The portion of shell prior the line was formed during the acclimation phase. dog =  
 787 direction of growth. The Raman spectral maps indicate the ratio  $R_{v1/Ta}$  for each data point of the scan. For

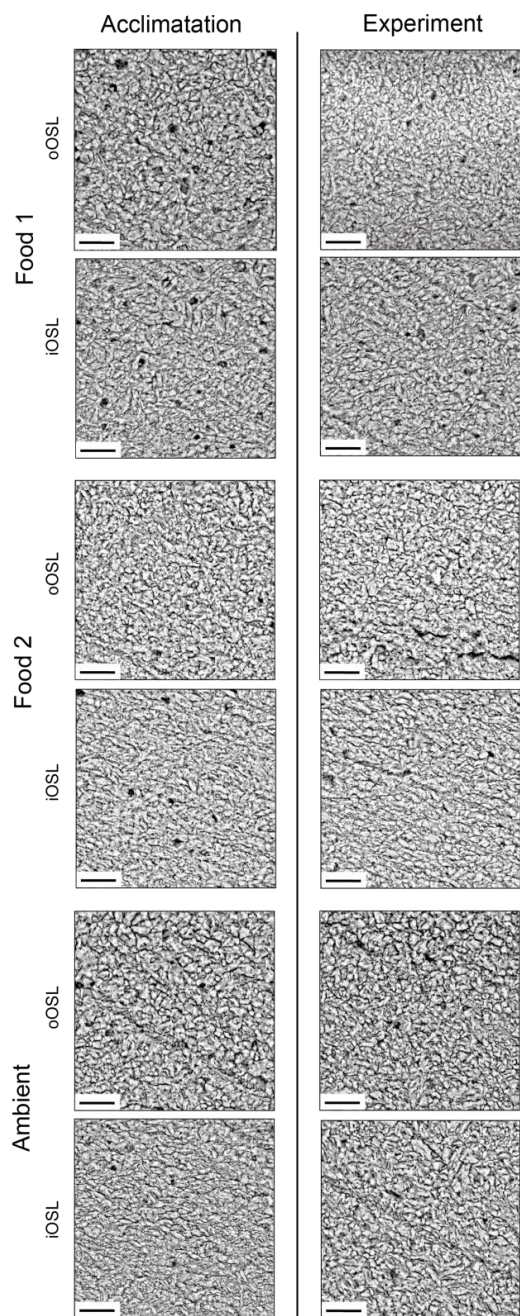


788 each shell, maps on the left represent shell portions during the experiment, maps on the right represent shell  
789 portions formed during the acclimation phase. In the acclimation portion of the sample reared with ambient  
790 food, a significant change in the microstructure orientation is visible. The respective area of the Raman map  
791 was not considered in further calculations because it was influenced by the emersion and transportation  
792 stress at the start of the experiment. Scale bars = 10  $\mu\text{m}$ . The graphs show the proportions of biominerals of  
793 oOSL and iOSL with  $R_{\text{vI/Ta}} > 2.5$  a.u. with respect to the total map area.

794

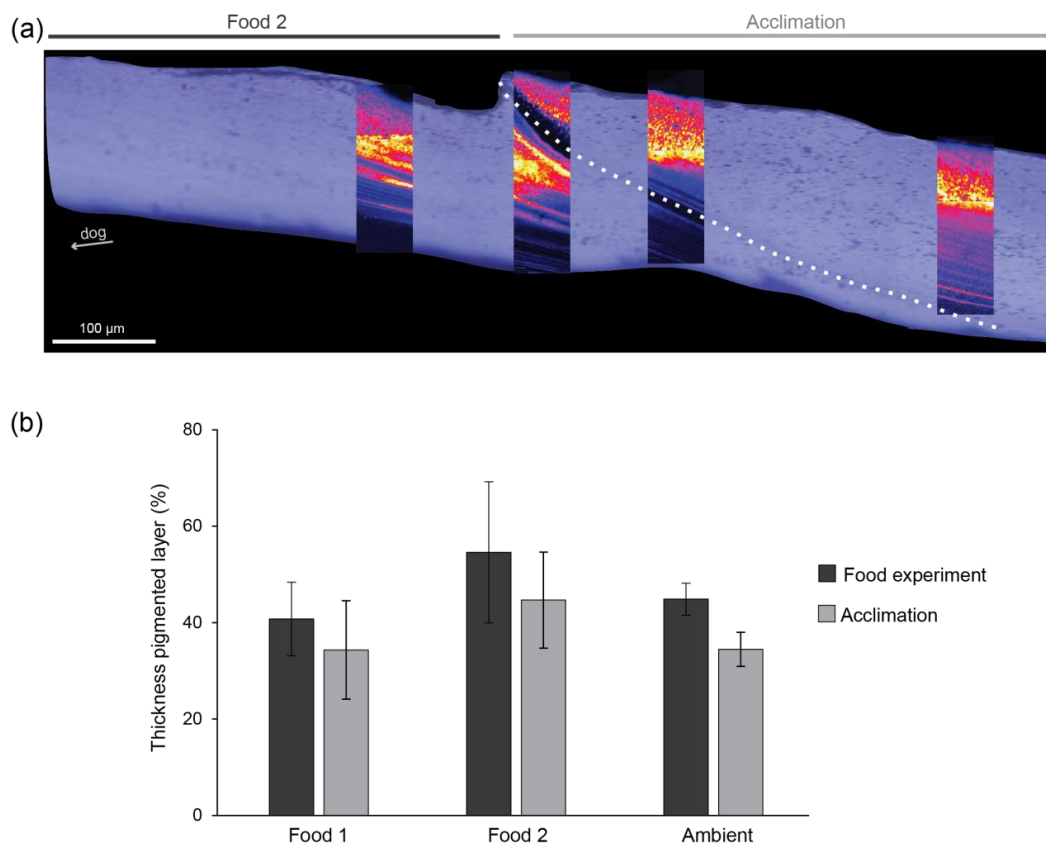
795





796

797 **Fig. 7.** SEM images of *Arctica islandica* shell microstructures formed during the acclimation phase at AWI  
798 (left column) and during the food experiment (right column). Scale bars = 4  $\mu\text{m}$ .



799

800 **Fig. 8.** Effects of diet on shell pigment distribution. (a) Raman spectral maps of the 1524 cm<sup>-1</sup> band  
801 representing the distribution of the polyenes in the shell cultured with food type 2. Dotted line marks the  
802 start of the experiment. dog = direction of growth. (b) The graph shows the thickness of the pigmented layer  
803 over the whole shell thickness before and during the food experiments.

804

805


 806 **Table 1.** List of the studied specimens of *Arctica islandica* and experimental conditions.

Sample ID	Locality	Age	Experiment	Treatment
A2	Maine	5	Temperature	10 °C + 15 °C <sup>807</sup>
A4	Maine	4	Temperature	10 °C + 15 °C
A5	Maine	4	Temperature	10 °C + 15 °C <sup>808</sup>
S12	Kiel Bay	1	Diet	Food 1
S14	Kiel Bay	1	Diet	Food 1 <sup>809</sup>
S15	Kiel Bay	1	Diet	Food 1
G11	Kiel Bay	1	Diet	Food 2 <sup>810</sup>
G12	Kiel Bay	1	Diet	Food 2
G15	Kiel Bay	1	Diet	Food 2 <sup>811</sup>
N13	Kiel Bay	1	Diet	No additional food
N15	Kiel Bay	1	Diet	No additional food <sup>812</sup>

813

 814 **Table 2.** Details of the pigment composition of the *Arctica islandica* shells used in the food experiment.

 815 The position of the major polyene peaks  $R_1$  and  $R_4$  in the Raman spectrum is indicated together with the

 816 number of single and double carbon bonds of the pigment molecular chain ( $N_1$  and  $N_4$ ). Each shell was

817 analyzed in the portions formed before and during the experimental phase.

Sample ID	Shell portion	$R_1$ (cm <sup>-1</sup> )	$R_4$ (cm <sup>-1</sup> )	$N_1$	$N_4$
S12	Acclimation	1130.9	1515.2	9.7	10.8
	Food 1	1121.4	1515.3	12.1	10.7
S14	Acclimation	1133.2	1519.4	9.3	10.2
	Food 1	1132.2	1518.6	9.5	10.3
S15	Acclimation	1129.5	1516.5	10.0	10.6
	Food 1	1132.1	1519.8	9.5	10.1
G11	Acclimation	1132.6	1518.4	9.4	10.3
	Food 2	1129.5	1517.0	10.0	10.5
G12	Acclimation	1131.7	1518.7	9.6	10.3
	Food 2	1132.1	1518.2	9.5	10.4
G15	Acclimation	1132.4	1519.5	9.4	10.2
	Food 2	1128.0	1520.9	10.3	10.0
N13	Acclimation	1130.2	1515.6	9.9	10.7
	Ambient food	1131.4	1514.1	9.6	10.9
N15	Acclimation	1117.9	1516.0	13.3	10.6
	Ambient food	1130.7	1517.0	9.8	10.5
Average		1129.7 ± 4.2	1517.5 ± 2.0	10.1 ± 1.1	10.4 ± 0.3

818